Efficient Resource Allocation for All-Optical Multicasting Over Spectrum-Sliced Elastic Optical Networks

Long Gong, Xiang Zhou, Xiahe Liu, Wenwen Zhao, Wei Lu, and Zuqing Zhu

***Abstract*—Recently, optical orthogonal frequency-division multiplexing technology has attracted intensive research interest because spectrum-sliced elastic optical networks (EONs) can be constructed based on it. In this paper, we investigate how to serve multicast requests over EONs with multicast-capable routing, modulation level, and spectrum assignment (RMSA). Both EON planning with static multicast traffic and EON provisioning with dynamic traffic are studied. For static EON planning, we formulate two integer linear programming (ILP) models, i.e., the joint ILP and the separate ILP. The joint ILP optimizes all multicast requests together, while the separate ILP optimizes one request each time in a sequential way. We also propose a highly efficient heuristic that is based on an adaptive genetic algorithm (GA) with minimum solution revisits. The simulation results indicate that the ILPs and the GA provide more efficient EON planning than the existing multicast-capable RMSA algorithms that use the shortest path tree (SPT) and the minimal spanning tree (MST). The results also show that the GA obtains more efficient EON planning results than the separate ILP with much less running time, as it can optimize all multicast requests together in a highly efficient manner. For the dynamic EON provisioning, we demonstrate that the GA is also applicable, and it achieves lower request blocking probabilities than the benchmark algorithms using SPT and MST.

***Index Terms*—Adaptive genetic algorithm; Multicast traffic; Optical orthogonal frequency-division multiplexing (O-OFDM); Routing, modulation-level, and spectrum assignment (RMSA).**

I. INTRODUCTION

Recent advances in optical orthogonal frequency-division multiplexing (O-OFDM) technology have demonstrated efficient and elastic bandwidth allocation in the optical layer [1,2]. O-OFDM grooms the capacities of several contiguous narrowband subcarrier frequency slots and achieves ultra-high-speed data transmission over them [2]. Since a bandwidth-variable O-OFDM transponder can adjust the number of subcarrier slots and assign just-enough spectral resource to each connection request

[3], people have tended to refer optical transport networks based on O-OFDM as spectrum-sliced elastic optical networks (EONs) [4]. In EONs, the fundamental problem of network planning and provisioning is routing and spectrum assignment (RSA). When RSA becomes impairment aware, an O-OFDM transponder can make the modulation level of its subcarrier slots be adaptive to the quality of transmission of a lightpath [5,6]. Therefore, impairment-aware RSA is essentially a routing, modulation-level, and spectrum assignment (RMSA) problem.

Given a set of connection requests, the network planning problem of setting up lightpaths with RSA or RMSA is known as NP-complete [7]. This problem is also considered a static one, since all requests are known *a priori*. Previous work has already proposed several integer linear programming (ILP) models and heuristic algorithms to solve the problem of EON planning [7–10]. EON provisioning considers how to serve time-variant connection requests in a dynamic network environment. Several dynamic RSA/RMSA algorithms have also been recently proposed for EON provisioning [11–13].

Nevertheless, none of the previous work mentioned above considered multicast traffic. Note that multicast is widely used to support applications, such as teleconferencing, IP television, and stock exchanges, and it is contributing an important portion to Internet traffic. Moreover, there is recently a growing demand to support scientific applications that can transfer huge amounts of data to a few geographically dispersed users [14]. Because it can reduce repeated optical–electrical–optical conversions to the maximum extent practicable, all-optical multicasting leads to more transparent and power-efficient solutions compared to conventional IP multicasting [15–17]. For all-optical multicasting in wavelength-division multiplexing (WDM) networks, previous studies have investigated the routing and wavelength assignment problem in [18,19], the multicast-capable switch architectures in [17,20,21], multicast overlay network designs in [22], etc. Since the O-OFDM technology can achieve more flexible bandwidth allocation in the optical layer, we expect the EONs to provide more efficient support for all-optical multicasting scenarios, especially when traffic demands dynamically vary a lot. Therefore, we investigate how to serve multicast

requests over EONs with multicast-capable RMSA in this work. Recently, Wang and Chen performed a performance analysis of two RSA algorithms that could support multicast traffic [23]. The multicast-capable RSA algorithms were designed to use either the shortest path tree (SPT) [24] or the minimal spanning tree (MST) [25]. However, the proposed SPT and MST algorithms did not consider adaptive modulation-level assignment. Moreover, as we will show below, the solutions they obtained were suboptimal. Yu *et al.* considered modulation-level changes at the nodes and studied multicast RMSA in translucent EONs where optical–electrical–optical conversions are permitted in the light trees [26].

In this paper, we first investigate EON planning with multicast traffic and formulate two ILP models, i.e., the joint ILP and separate ILP. The joint ILP optimizes all multicast requests together, while the separate ILP optimizes one request at a time and handles the requests sequentially. To reduce the computational complexity, we also propose a highly efficient heuristic that is based on an adaptive genetic algorithm (GA) that minimizes solution revisits. EON provisioning with dynamic multicast traffic is studied afterward. With numerical simulations, we demonstrate that the GA is also applicable to the dynamic provisioning and that it outperforms the existing multicast-capable RMSA algorithms by providing lower request blocking probabilities.

The rest of the paper is organized as follows. For EON planning, the problem is defined in Section II, the two ILP models are formulated in Section III, the adaptive GA is discussed in Section IV, and the performance evaluation is presented in Section V. For EON provisioning, the problem definition and the GA-based RMSA algorithm is discussed in Section VI, and the performance evaluation is presented in Section VII. Finally, Section VIII summarizes the paper.

II. EON PLANNING WITH STATIC MULTICAST TRAFFIC

In this section, we discuss the network model and RMSA procedures for the network planning that supports all-optical multicasting in EONs. In this case, all multicast requests are known *a priori* for this static EON planning, and they all have to be accommodated in the EON simultaneously; i.e., we do not allow request blocking.

A. Network Model

We consider a physical network topology as $G(V, E)$, where V is the node set and E is the fiber link set. We assume that the bandwidth of each subcarrier slot is the same and that each fiber link can accommodate B slots at most. The capacity of one subcarrier slot is C_{slot}^{BPSK} in gigabits/second, when the modulation is binary phase-shifted keying (BPSK). Let m be the modulation level in terms of bits per symbol, e.g., for BPSK, $m = 1$. Hence, the capacity of one slot is $m \cdot C_{slot}^{BPSK}$ for different modulation levels. In this paper, we assume that m can be 1, 2, 3, and

4 for BPSK, quadrature phase-shifted keying (QPSK), 8-QAM, and 16-QAM, respectively. When the modulation level of an O-OFDM signal becomes higher with more bits per symbol (e.g., changing from BPSK to QPSK), its transmission reach decreases owing to lower receiver sensitivity [5].

B. RMSA Procedures for Multicast Requests

In the context of this work, we assume that there is no spectrum conversion in the EON and that each node has a multicast-capable optical cross connect that is based on splitter-and-delivery switches [20]. With the splitter-and-delivery switches, we incorporate the same-spectrum multicast scheme in Fig. 1(a), similar to the same-wavelength scheme in WDM networks [24]. Let $MR_i = \{s_i, D_i, C_i\}$ denote a multicast request, where i is its unique ID, s_i is the source node, D_i is the destination node set, and C_i is the requested capacity. The procedures of multicast-capable RMSA are as follows.

1) Multicast Routing: We first determine the multicast tree, i.e., the light tree [15] for each multicast request. Specifically, We consider the light tree as the combination of the routing paths from s_i to each destination $d_{i,j} \in D_i$, $j = 1, 2, ..., |D_i|$ and obtain a multicast path set $\{R_{s_i, d_{i,j}}, \forall\, d_{i,j} \in D_i\}$ to construct the corresponding light tree $\mathcal{T}_i$. In this paper, we assume that there is no limitation on the number of branching points in each multicast light tree.

2) Modulation-Level Selection and Spectrum Assignment: After constructing the light tree, we determine the modulation level and assign the spectrum. For each
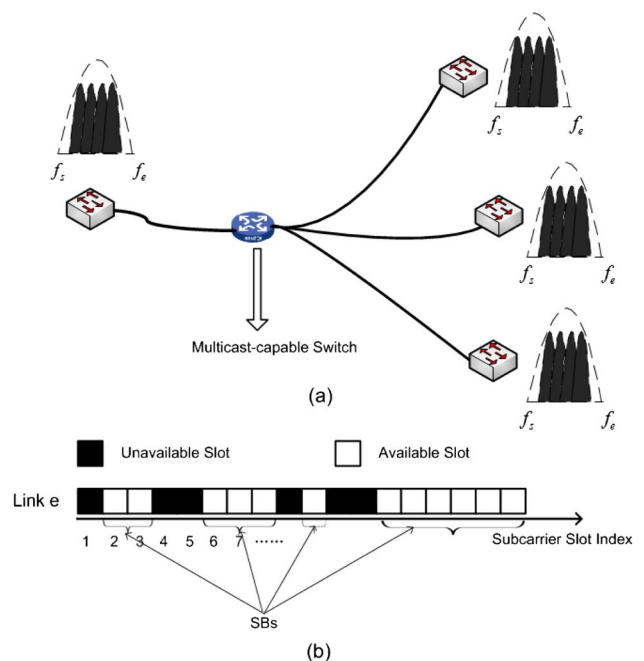

Fig. 1.   (a) Same-spectrum multicast scheme and (b) definition of slot block (SB) on EON links.

multicast path, we can derive a modulation level based on its transmission distance. Specifically, we assume that each modulation level can support a maximum transmission distance based on the receiver sensitivities [5,6], and when the distance permits, we always choose the highest modulation level m_p for the highest spectral efficiency. In this paper, we assume that the majority of the impairments are from the long-distance transmission between the nodes and that the impairments caused by the intermediate nodes are relatively small and can be compensated with a performance margin preset according to the worst-case scenario. Note that the impairment-aware modulation-level selection scheme would be more practical if we consider the impairments at the intermediate nodes, especially the additional impairments due to optical splitting at the branching nodes. We will address this in our future work and expect that it can be resolved with a more sophisticated performance model that considers the physical layer impairments more comprehensively [27]. We obtain the number of contiguous slots n_p to be assigned on the multicast path as follows:

$$n_p = \left\lceil \frac{C_i}{m_p \cdot C_{\text{slot}}^{\text{BPSK}}} \right\rceil + N_{\text{GB}}, \qquad (1)$$

where N_{GB} is the fixed number of slots for the guard band. Note that recent work has shown that the guard band can be adaptive to the modulation-level assignment [28]. However, the assumption here about the fixed N_{GB} would not limit the effectiveness of our approaches. Basically, when C_i and $C_{\text{slot}}^{\text{BPSK}}$ are given, n_p is still a function of m_p in Eq. (1), even if N_{GB} can change with m_p. Therefore, by modifying Eq. (1) to $n_p = \lceil C_i / m_p \cdot C_{\text{slot}}^{\text{BPSK}} \rceil + N_{\text{GB}}(m_p)$, our approaches can adapt to the scenarios in which N_{GB} is not fixed.

In order to comply with the same-spectrum scheme, the modulation level m_i of MR$_i$ has to be the same on different multicast paths. Therefore, we derive m_i of MR$_i$ based on the transmission distance of the longest routing path in the multicast path set $\{R_{s_i,d_{i,j}}, \forall\, d_{i,j} \in D_i\}$, which is equivalent to assigning the contiguous slots according to the longest routing path; i.e., the number of contiguous slots to be assigned to the multicast request MR$_i$ is

$$n_i = \max n_p, \quad \forall\, p \in \{R_{s_i,d_{i,j}}, \forall\, d_{i,j} \in D_i\}. \qquad (2)$$

III. ILP Formulations for EON Planning With Static Multicast Traffic

In this section, we formulate two ILP models to solve the network planning for EONs with multicast traffic. Both of the ILP models are based on routing paths and slot blocks (SBs); i.e., they find the multicast paths and the starting slots of the SBs on them to minimize the spectrum usage. A SB is defined below, and an intuitive example of SBs can be found in Fig. 1(b).

Definition 3.1 (slot block). A SB is a block of a few available contiguous subcarrier slots in the optical spectrum.

Definition 3.2 (maximal slot block). A maximal SB (MSB) is a SB to which we cannot add any other available slot such that its slots remain contiguous.

A. Joint ILP Formulation

The joint ILP considers all multicast requests together and tries to obtain the optimal solution for EON planning.

Notations:
- $G(V,E)$: the physical topology.
- $\{\text{MR}_i, i \in I\}$: the set of multicast requests.
- s_i: the source node of MR$_i$.
- D_i: the destination node set of MR$_i$.
- $d_{i,j}$: the jth destination in D_i.
- C_i: the requested capacity of MR$_i$.
- B: the number of subcarrier slots on each fiber link.
- K: the number of path candidates for each s–d pair.
- P: the set of all routing path candidates in $G(V,E)$ for RMSA optimization.
- $P_{s,d}^V$: the set of K routing path candidates that are from node s to d, $s, d \in V$, $P = \bigcup_{s,d \in V} P_{s,d}^V$.
- P_e^E: the set of routing path candidates that use link $e \in E$.
- m_p: the highest modulation level that can be supported by path p, $p \in P$.
- n_p: the number of contiguous slots according to the highest modulation level of the path $p \in P$; it is predetermined by Eq. (1).

The above notation denotes the inputs to the joint ILP. We make B reasonably large to prevent request blocking. We obtain m_p for each $p \in P$ based on its transmission distance.

Variables:
- $x_{p,i}$: Boolean variable that equals 1 if path p is used for request MR$_i$, and 0 otherwise.
- $y_{e,i}$: integer variable that indicates the number of times that link e is used for request MR$_i$.
- $o_{i,j}$: Boolean variable that equals 1 if the starting slot of request MR$_i$ is smaller than that of request MR$_j$, and 0 otherwise.
- $c_{i,j}$: Boolean variable that equals 1 if requests MR$_i$ and MR$_j$ use common link(s), and 0 otherwise.
- w_i: integer variable that indicates the SB's starting slot for request MR$_i$.
- z_i: integer variable that indicates the SB's ending slot for request MR$_i$.
- n_i: integer variable that indicates the number of subcarrier slots on a link to serve MR$_i$, i.e., the size of the SB used for MR$_i$.

Objective:

$$\text{Minimize} \max_i (z_i), \quad \forall\, i \in I. \qquad (3)$$

The objective of the joint ILP is to minimize the maximum ending slot index of all multicast requests $\{MR_i, i \in I\}$. In order to make the objective function linear, we define another variable T and add a constraint to the joint ILP:

$$z_i \leq T, \quad \forall\, i \in I. \tag{4}$$

Then, the objective function becomes

$$\text{Minimize } T. \tag{5}$$

As the network operator usually determines how many subcarrier slots he/she should allocate on each fiber link based on T, the objective function in Eq. (5) leads to efficient spectrum utilization for EON planning.

Constraints:

1) Light-tree construction:

$$\sum_{p \in P^V_{s_i, d_{i,j}}} x_{p,i} = 1, \quad \forall\, d_{i,j} \in D_i, \quad \forall\, i \in I. \tag{6}$$

Equation (6) ensures that for each multicast request MR_i, the connection from s_i to each $d_{i,j}$ is routed over a single path:

$$y_{e,i} \geq x_{p,i}, \quad \forall\, i \in I, \quad \forall\, p \in P^E_e \cap P^V_{s_i, d_{i,j}}, \quad \forall\, e \in E,$$
$$\forall\, d_{i,j} \in D_i, \tag{7}$$

$$y_{e,i} \leq 1, \quad \forall\, i \in I, \quad \forall\, e \in E. \tag{8}$$

Equations (7) and (8) ensure that for each selected routing path p, all links on it are handled and are considered just once.

2) Modulation-level selection:

$$n_i \geq n_p \cdot x_{p,i}, \quad \forall\, p \in P^V_{s_i, d_{i,j}}, \quad \forall\, d_{i,j} \in D_i, \quad \forall\, i \in I. \tag{9}$$

As stated above, Eq. (9) ensures the modulation level of the corresponding multicast request can support the transmission distances of all multicast paths that are selected for this request.

3) Spectrum assignment:

$$c_{i,j} \geq y_{e,i} + y_{e,j} - 1, \quad \forall\, i,j \in I, i \neq j, \quad \forall\, e \in E. \tag{10}$$

Equation (10) ensures that all common links between any two different requests MR_i and MR_j are handled:

$$o_{i,j} + o_{j,i} = 1, \quad \forall\, i,j \in I, i \neq j. \tag{11}$$

$$z_j - w_i + 1 \leq B \cdot (1 + o_{i,j} - c_{i,j}), \quad \forall\, i,j \in I, i \neq j. \tag{12}$$

$$z_i - w_j + 1 \leq B \cdot (2 - o_{i,j} - c_{i,j}), \quad \forall\, i,j \in I, i \neq j. \tag{13}$$

Equations (11)–(13) ensure that the spectrum assignments of any two different requests MR_i and MR_j are

not overlapped with each other in the spectrum domain:

$$z_i - w_i + 1 \geq n_i, \quad \forall\, i \in I. \tag{14}$$

Equation (14) ensures that the requested capacity of each multicast request is satisfied.

4) Variable range:

$$w_i, z_i, T \in (0, B], \quad \forall\, i \in I. \tag{15}$$

Equation (15) limits the variable ranges of w_i, z_i, and T.

For each multicast request in $\{MR_i, i \in I\}$, the joint ILP finds the multicast paths (i.e., $x_{p,i} = 1$) or the light tree (i.e., the tree determined by $y_{e,i} = 1$), and the SBs (determined by w_i and z_i) for data transmission. Then, we determine the modulation level m_i used to serve MR_i as

$$m_i = \min m_p, \qquad \{p : x_{p,i} = 1\}. \tag{16}$$

Finally, multicast-capable RMSA is solved for all multicast requests.

B. Separate ILP Formulation

Even though the joint ILP can optimize multicast-capable RMSA for EON planning, its computational complexity is also relatively high. As we will show below in the simulation results, it is not scalable to large problems, i.e., if the network size is large and/or the multicast requests are many. We therefore decompose the EON planning of all multicast requests into a few subproblems, each of which solves the RMSA of one multicast request with an ILP. With this approach, the computational complexity can be reduced greatly. We refer to this approach as "separate ILP," in which the multicast requests $\{MR_i\}$ are first sorted in descending order based on their capacities $\{C_i\}$, and then a few ILPs are solved sequentially to find the RMSA solutions of $\{MR_i\}$ one by one.

Notations:

- $G(V, E)$: the physical topology.
- MR_i: a multicast request.
- D_i: the destination node set of MR_i.
- $d_{i,j}$: the jth destination in D_i.
- B: the number of subcarrier slots on each fiber link.
- K: the number of path candidates for each s–d pair.
- P: the set of all routing path candidates in $G(V, E)$ for the RMSA optimization.
- $P^V_{s,d}$: the set of K routing path candidates that are from node s to d, $s, d \in V$, $P = \bigcup_{s,d \in V} P^V_{s,d}$.
- P^E_e: the set of routing path candidates that use link $e \in E$.
- m_p: the highest modulation level that can be supported by path p, $p \in P$.
- $w_{e,k}$: the starting slot of the kth MSB on link e.
- $z_{e,k}$: the ending slot of the kth MSB on link e.

- n_p: the number of contiguous slots according to the highest modulation level of the path $p \in P$; it is predetermined by Eq. (1).

The above notation denotes the inputs to each separate ILP. As the notation of the parameters of MR_i, such as s_i and C_i is the same as in the joint ILP, we do not list those terms again. Also, the routing path set P is determined with the same methods. Note that after each ILP, we update $w_{e,k}$ and $z_{e,k}$ on each link $e \in E$ to record the spectrum utilization.

Variables:
- x_p: Boolean variable that equals 1 if path $p \in P$ is used for MR_i, and 0 otherwise.
- $u_{e,k}$: Boolean variable that equals 1 if the kth MSB on link e is used for MR_i, and 0 otherwise.
- y_e: integer variable that indicates the number of times that link e is used for request MR_i.
- w: integer variable that indicates the SB's starting slot for request MR_i.
- z: integer variable that indicates the SB's ending slot for request MR_i.
- n_i: integer variable that indicates the number of subcarrier slots on a link to serve MR_i.

Objective:

$$\text{Minimize} \, z \tag{17}$$

Constraints:
1) Light-tree construction:

$$\sum_{p \in P^V_{s_i, d_{i,j}}} x_p = 1, \quad \forall \, d_{i,j} \in D_i. \tag{18}$$

Equation (18) ensures single-path routing for the connection from s_i to each $d_{i,j}$:

$$y_e \geq x_p, \quad \forall \, e \in E, \quad \forall \, p \in P^E_e, \tag{19}$$

$$y_e \leq 1, \quad \forall \, e \in E. \tag{20}$$

Equations (19) and (20) ensure that for each selected routing path p, all links on it are handled and are considered just once.

2) Modulation-level selection:

$$n_i \geq n_p \cdot x_p, \quad \forall \, p \in P^V_{s_i, d_{i,j}}, \quad \forall \, d_{i,j} \in D_i, \quad \forall \, i \in I. \tag{21}$$

As stated above, Eq. (21) ensures the modulation level m_i can support the transmission distances of all multicast paths that are selected.

3) Spectrum assignment:

$$w \geq w_{e,k} \cdot u_{e,k}, \quad \forall \, e \in E, \quad \forall \, k, \tag{22}$$

$$z \leq (z_{e,k} - B) \cdot u_{e,k} + B, \quad \forall \, e \in E, \quad \forall \, k. \tag{23}$$

Equations (22) and (23) ensure that the assigned spectrum falls in the kth MSB on link e, when the MSB is used for MR_i:

$$z - w + 1 \geq n_i, \quad \forall \, p \in P. \tag{24}$$

Equation (24) ensures that the requested capacity of MR_i is satisfied:

$$\sum_k u_{e,k} = y_e, \quad \forall \, e \in E. \tag{25}$$

Equation (25) ensures that MR_i is served with only one SB on any links that are used.

4) Variable range:

$$w, z \in (0, B]. \tag{26}$$

Equation (26) limits the variable ranges of w and z.

For each multicast request in $\{MR_i, i \in I\}$, the above separate ILP finds the multicast paths (i.e., $x_p = 1$) or light tree (i.e., the tree determined by $y_e = 1$) and the SB (determined by w and z) on them for data transmission, based on the current network status, i.e., $\{w_{e,k}, z_{e,k}, \forall \, e \in E\}$. Similar to the joint ILP, the modulation level used to serve the multicast request is determined as

$$m = \min m_p, \qquad \{p : x_p = 1\}. \tag{27}$$

Note that the separate ILP can optimize the RMSA solution for each multicast request based on the current network status, but since the requests are handled one-by-one, the overall RMSA solution may not be optimal for all multicast requests.

IV. ADAPTIVE GENETIC ALGORITHM FOR EON PLANNING WITH STATIC MULTICAST TRAFFIC

It is known that ILP models are not scalable to large problems. In this section, we propose a highly efficient heuristic that incorporates an adaptive GA for EON planning with multicast traffic. Previously, we have proposed two GAs to solve EON planning [9] and provisioning [29] problems for EONs with unicast traffic. Since the scheme with multicast traffic is intrinsically more complicated than that with unicast traffic, we improve the GA from three perspectives to make it more efficient. 1) We modify the genetic encoding scheme to accommodate multicast requests. 2) We design the crossover and mutation operations with adaptive schemes to improve the GA's search efficiency. 3) We introduce a mechanism to minimize the redundant computation time on solution revisits;

i.e., the GA computes the same RMSA solution more than once.

A. Genetic Encoding and Objective

GA is an optimization strategy that mimics the natural evolution [30]. For EON planning with multicast traffic, a feasible RMSA solution for all multicast requests is encoded as a set of genes, called an individual chromosome (or individual). In order to encode the genes for multicast requests, we decompose $MR_i = \{s_i, D_i, C_i\}$ into a set of correlated unicast requests, i.e., $\{\{s_i, d_{i,j}, C_i\}, d_{i,j} \in D_i\}$. Let $P_{s,d}^V$ denote the set of routing path candidates that are from node s to d, $s, d \in V$. After request decomposition, we randomly select a feasible routing path $R_{s_i,d_{i,j}}$ from $P_{s_i,d_{i,j}}^V$ for each correlated unicast request, $\{s_i, d_{i,j}, C_i\}$. Then, the modulation level m_i and the number of contiguous slots n_i on each multicast path can be determined with the procedures discussed in Subsection II.B, to comply with the same-spectrum multicast scheme. We define a bit mask a_i with B bits to assist the spectrum assignment of MR_i; in particular $a_i[k] = 1$ means the kth slot is assigned to MR_i, otherwise, $a_i[k] = 0$. Finally, the RMSA solution of MR_i is expressed as $\{\{R_{s_i,d_{i,j}}, d_{i,j} \in D_i\}, m_i, a_i\}$, and it is encoded as a gene $\mathcal{G}_i = \{\{R_{s_i,d_{i,j}}, d_{i,j} \in D_i\}, m_i, a_i\}$.

In a GA, a gene refers to a feasible solution to a subproblem, while an individual (i.e., a set of all genes) represents a feasible solution to the problem. Hence, after repeating the above procedures for all $|I|$ multicast requests $\{MR_i, i \in I\}$, we form an individual $\mathcal{I}$ that contains $|I|$ genes. We can select different routing paths for some or all of the genes to form different individuals, and the set of individuals $\mathcal{I}$ is the population $\mathcal{P}$ in the GA.

The objective function of the GA is the same as that of the joint ILP, i.e., Eq. (5) in Subsection III.A. More specifically, for each individual $\mathcal{I}$, we obtain T with Eq. (4) and assign its fitness as T. In the GA, individuals with smaller T have a larger probability to survive.

B. Adaptive Genetic Operations

We elaborate on the details of the adaptive genetic operations in this subsection. Based on the individuals' fitness, the GA implements typical genetic operations, including selection, crossover, and mutation in iterations (i.e., evolution generations), to optimize EON planning.

We design the selection operation with tournament selection [31] to select pairs of individuals (e.g., parents) from the current generation for crossover. Tournament selection involves running several tournaments among a fixed number of individuals that are randomly chosen from the population. The winner of each tournament, i.e., the fittest one in the group, is selected. We then take pairs randomly from the selected individuals and let them cross over to generate offspring. The crossover is a multipoint operation on the gene level, in which a few genes in the parents are selected randomly and swapped. The actual number of

genes to swap is calculated with $\lceil |I| \cdot p_c \rceil$, where p_c is the crossover rate. In the next step, we select $|\mathcal{P}|$ fittest individuals from the chromosome pool of parents and offspring as the new generation, while keeping the population size constant during the evolution. These individuals then go through the mutation phase, in which they have some of their genes modified randomly. Similarly, the number of genes to mutate in each individual is calculated with $\lceil |I| \cdot p_m \rceil$, where p_m is the mutation rate. Specifically, we mutate a gene $\mathcal{G}_i$ by modifying its RMSA to other feasible ones randomly.

In order to achieve high-efficiency for the GA, we adopt an adaptive mechanism to adjust p_c and p_m dynamically based on the individuals' fitness. Let the population be denoted $\mathcal{P} = \{\mathcal{I}_l\}$, $l = 1, \ldots, |\mathcal{P}|$, and T_l is the fitness of individual $\mathcal{I}_l$. We have $T_{\min} = \min_l(T_l)$, $T_{\text{mean}} = \sum_l T_l / |\mathcal{P}|$, and $\bar{T}_{l_1,l_2} = (T_{l_1} + T_{l_2})/2$. Then, p_c and p_m are calculated as [32]

$$p_c = \begin{cases} \alpha_c \frac{\bar{T}_{l_1,l_2} - T_{\min}}{T_{\text{mean}} - T_{\min}} + p_{c_0}, & \bar{T}_{l_1,l_2} \leq T_{\text{mean}}, \\ \beta_c, & \text{otherwise} \end{cases} \quad (28)$$

$$p_m = \begin{cases} \alpha_m \frac{T_l - T_{\min}}{T_{\text{mean}} - T_{\min}} + p_{m_0}, & T_l \leq T_{\text{mean}}, \\ \beta_m & \text{otherwise} \end{cases} \quad (29)$$

where α_c, β_c, α_m, and β_m are constant coefficients $\in [0, 1]$, and p_{c_0} and p_{m_0} are the default rates for the fittest individuals in the population.

After crossover and mutation, we introduce a mechanism to minimize individual revisits. Specifically, when calculating the fitness of each individual in the new generation, we skip redundant computation if an individual has already been visited. This can greatly improve the efficiency of the GA, as when the GA converges, the population consists of more and more identical individuals with relatively good fitness.

C. Algorithm Convergence Condition

To evaluate the GA's convergence performance, we define its degree of diversity as [9]

$$D_P = \frac{2}{|\mathcal{P}|(|\mathcal{P}| - 1)} \sum_{l_1=1}^{|\mathcal{P}|-1} \sum_{l_2=l_1+1}^{|\mathcal{P}|} \frac{d(l_1, l_2)}{|I|}, \quad (30)$$

where $d(l_1, l_2)$ returns the number of different genes between individuals $\mathcal{I}_{l_1}$ and $\mathcal{I}_{l_2}$. We can claim that the GA has converged if D_P has been lower than a preset threshold for a certain number of generations or more [30].

Algorithm 1 illustrates the procedures of the proposed adaptive GA for EON planning with multicast-capable RMSA.

Algorithm 1 Adaptive GA for EON Planning With Multicast-Capable RMSA

1: $\mathcal{P} = \varnothing$;
   {Phase I: Construct Initial Populations $\mathcal{P}$}
2: **while** $|\mathcal{P}|$ is not large enough **do**
3:   $\mathcal{I} = \varnothing$;
     {Construct an Individual Chromosome $\mathcal{I}$}
4:   **for** all requests MR_i **do**
5:     decompose MR_i into $\{\{s_i, d_{i,j}, C_i\}, d_{i,j} \in D_i\}$;
6:     select $\{R_{s_i,d_{i,j}}\}$ from $\bigcup_{d_{i,j} \in D_i} P^V_{s_i,d_{i,j}}$ randomly;
7:     select m_i based on $\{R_{s_i,d_{i,j}}\}$;
8:     calculate n_i based on m_i and C_i;
9:     construct a gene $\mathcal{G}_i = \{\{R_{s_i,d_{i,j}}, d_{i,j} \in D_i\}, m_i\}$;
10:     insert $\mathcal{G}_i$ into $\mathcal{I}$;
11:   **end for**
12:   insert $\mathcal{I}$ into $\mathcal{P}$;
13: end **while**
     {Phase II: Evolution}
14: $\mathcal{I}_{\text{best}} = \varnothing$;
15: **while** GA has not converged do
16:   **for** all $\mathcal{I}$ in $\mathcal{P}$ **do**
17:     **if** $\mathcal{I}$ is not a revisited solution **then**
18:       find $\{a_i\}$ for all genes $\{\mathcal{G}_i\}$ in $\mathcal{I}$;
19:       calculate fitness T for $\mathcal{I}$;
20:     **end if**
21:   **end for**
22:   $\mathcal{I}_{\text{best}} \leftarrow$ the fittest one in $\mathcal{P}$;
23:   evolve $\mathcal{P}$ for one generation with adaptive crossover and mutation;
24:   calculate the degree of diversity $D_{\mathcal{P}}$ for $\mathcal{P}$;
25: **end while**

V. Performance Evaluation of EON Planning With Static Multicast Traffic

We evaluate the proposed multicast-capable RMSA algorithms with simulations using the 14-node NSFNET topology (as shown in Fig. 2). Table I shows the simulation parameters. The transmission reach of each modulation level is determined based on the experimental results in [5]. The s_i and D_i of each MR_i are randomly selected. For each $s-d$ pair in the topology, we calculate four path candidates (i.e., $K = 4$). In addition to the joint ILP,
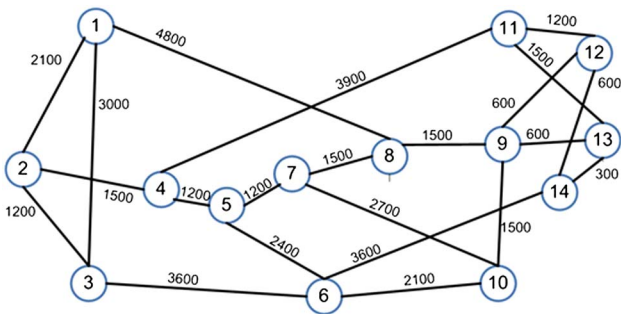

Fig. 2. NSFNET topology with fiber lengths in kilometers marked on each link.

separate ILP, and adaptive GA, we also implement two multicast-capable RMSA algorithms, based on the SPT and the MST [23], as the benchmark algorithms. For these two benchmark algorithms, the procedures are similar to that of the separate ILP; i.e., we first sort the multicast requests in descending order based on their capacities and then find the RMSA solutions for them one by one.

We use GLPK [33] to solve the ILPs and use MATLAB to implement the heuristic algorithms. All simulations are run on a computer with 3.1 GHz Intel Core i5-2400 CPU and 4 Gbytes RAM. Table II summarizes the simulation results on T (i.e., the maximum index of used slots on all links) and running time for different multicast traffic scenarios. For each traffic scenario, we run the simulations ten times with ten different request sets and record average values of T and running time. For the ILPs, we stop the simulations if the optimal solution for a traffic scenario cannot be obtained within 2 h.

It can be seen that the joint ILP achieves the most efficient EON planning by providing the smallest T. However, because of the high computational complexity, it consumes too much running time and becomes impractical when there are 10 or more multicast requests to plan in the NSFNET topology. For the schemes in which the requests are optimized sequentially (i.e., separate ILP, MST, and SPT), the separate ILP achieves the most efficient EON planning. But it can also become impractical when there are 50 or more requests to plan. This is because the computational complexity of the separate ILP depends heavily on the number of MSBs on the links (i.e., the numbers of $w_{e,k}$ and $z_{e,k}$), which increase dramatically with the number of requests, especially for requests that are handled toward the end of the EON planning.

It is interesting to note that the GA obtains better EON planning results (i.e., smaller T) than the separate ILP with much less running time. This is because, like the joint ILP, the GA optimizes all multicast requests together. Figure 3 shows the GA's convergence performance for EON planning with the heaviest traffic scenario in the simulations (i.e., $|I| = 100$, and average $|D_i|$ is 5). We observe that the GA has converged within 45 evolution iterations, which confirms the high efficiency of the GA. For the heaviest traffic scenario, the GA can optimize the 100 multicast requests in the NSFNET topology within 2.3270 s, or ~23 ms per request. We also observe that the running time of MST and SPT is much less than that of the GA. This is because both MST and SPT only calculate the RMSA once for each multicast request, while the GA tries multiple RMSAs and selects the best solution. In all, for all the traffic scenarios in the simulations, the GA reduces the average value of T by 12.7%–30.3%, 16.7%–42.5%, and 11.0%–42.1%, compared to the separate ILP, MST, and SPT, respectively.

VI. EON Provisioning With Dynamic Multicast Traffic

In this section, we investigate EON provisioning with dynamic multicast traffic, i.e., the requests are time

TABLE I
SIMULATION PARAMETERS

Bandwidth of a frequency slot	12.5 GHz
C_{slot}^{BPSK}, capacity of a slot using BPSK (i.e., $M = 1$)	12.5 Gbits/s
N_{GB}, number of slots for guard band per connection	1
K, number of path candidates for each $s-d$ pair	4
Transmission reach of BPSK ($m = 1$)	10,000 km
Transmission reach of QPSK ($m = 2$)	5000 km
Transmission reach of 8-QAM ($m = 3$)	2500 km
Transmission reach of 16-QAM ($m = 4$)	1250 km
Range of multicast request capacity (C_i)	10–100 Gbits/s
$|I|$, number of multicast requests to plan	5, 10, 50, 100
Average number of destinations per multicast request	2–5
$|\mathcal{P}| = 50$, population size of the GA	50
Threshold of D_P for GA convergence	0.15
Number of generations with D_P below the threshold to claim GA convergence	5
Number of request sets simulated for each data point	10

variant and can arrive and leave on the fly during network operation.

A. Network Model

Since it would be difficult to adjust network capacity (i.e., the number of slots per link or B) on the fly in dynamic provisioning [34], we have to fix B and consider request blocking when a feasible RMSA cannot be found under the capacity constraint. To emulate practical network provisioning [35], we assume that, at each discrete provision time, one or more pending multicast requests need to be served. The multicast requests arrive according to a Poisson process with an average arrival rate of λ requests per time unit, and the lifetime of each request follows the negative exponential distribution with an average of $1/\mu$ time units. Hence, the traffic load can be quantified with

λ/μ in erlangs. We say MR_i is blocked, if we cannot find a feasible RMSA $\{\{R_{s_i,d_{i.j}}, d_{i.j} \in D_i\}, n_i, a_i\}$ for it with the current network status. Note that we do not allow partial provisioning of a multicast request. Therefore, MR_i would be blocked even if we cannot serve only one destination in D_i. We define the objective of the EON provisioning such as to minimize the number of blocked requests.

B. Adaptive GA for EON Provisioning With Dynamic Multicast Traffic

Since EON provisioning is a real-time service, so that computation has to be done within each provision cycle, we need to make sure that the computation time is well controlled. In Table II, we observe that the GA's computation time for each request is around 23 ms even for the heaviest traffic scenario. We therefore believe that the

TABLE II
SIMULATION RESULTS FOR EON PLANNING WITH MULTICAST TRAFFIC

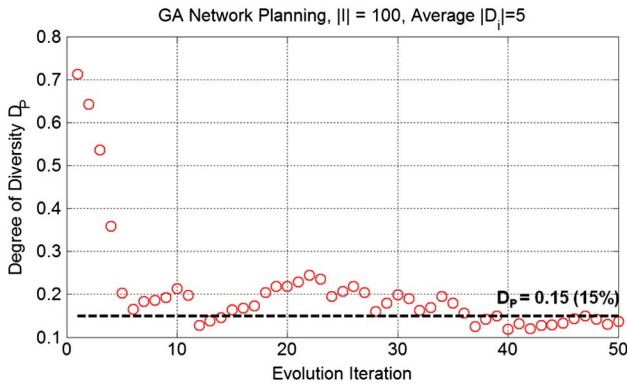| Traffic scenario		Joint ILP		Separate ILP		GA		MST		SPT	
$|I|$	Average $|D_i|$	Average T	Average running time (s)	Average T	Average running time (s)	Average T	Average running time (s)	Average T	Average running time (s)	Average T	Average running time (s)
5	2	7.1	26.4736	9.1	0.2798	7.1	0.1969	10.3	0.0038	10.3	0.0024
	3	7.4	203.2126	10.6	0.2718	7.7	0.2032	13.4	0.0040	13.3	0.0021
	4	7.9	717.5730	12.4	0.3200	9.3	0.2077	15.4	0.0050	14.1	0.0021
	5	8.2	1224.2689	12.6	0.3424	11.0	0.2166	13.2	0.0040	13.4	0.0031
10	2	—	—	15.1	0.5432	10.9	0.2368	15.5	0.0057	16.5	0.0033
	3	—	—	19.3	0.6149	13.9	0.2590	21.5	0.0048	21.3	0.0035
	4	—	—	25.1	0.7045	17.5	0.2844	29.2	0.0054	29.0	0.0041
	5	—	—	25.9	0.9100	19.1	0.3119	29.4	0.0055	28.6	0.0045
50	2	—	—	54.9	1904.0950	41.5	0.6930	62.6	0.0127	63.6	0.0124
	3	—	—	69.1	2360.8810	56.3	0.8381	73.8	0.0165	73.9	0.0155
	4	—	—	—	—	75.6	0.9734	101.2	0.0180	95.6	0.0177
	5	—	—	—	—	88.4	1.1110	112.2	0.0196	110.4	0.0217
100	2	—	—	—	—	79.0	1.3401	102.8	0.0240	104.8	0.0230
	3	—	—	—	—	116.1	1.6748	146.1	0.0338	141.4	0.0295
	4	—	—	—	—	137.7	2.0013	176.8	0.0358	160.1	0.0353
	5	—	—	—	—	177.8	2.3270	215.8	0.0412	199.7	0.0397

Fig. 3.   Convergence performance of adaptive GA for EON planning when the traffic scenario is $|I| = 100$ and average $|D_i|$ is 5.

adaptive GA can also be applicable to dynamic EON provisioning. More specifically, at each provision time, we run the GA once to optimize the multicast-capable RMSA for all pending requests.

To make the GA suitable for EON provisioning, we modify its objective function (or the fitness of each individual $\mathcal{I}$) to consider request blocking:

$$\text{Fitness} = T + H \cdot u(F_b) + F_b, \tag{31}$$

where T can be obtained with Eq. (4), $H \in \mathbb{N}^+$ is a large punishment coefficient to discourage RMSA solutions (i.e., individuals) that involve request blocking, $u(\cdot)$ is the unit step function that $u(x) = 1$ for $x > 0$, otherwise $u(x) = 0$, and F_b is the number of blocked requests caused by a RMSA solution. The objective of the GA is to minimize the fitness in Eq. (31) at any service provision time. Therefore, at each provision time, if the network is relatively empty and there is no request blocking, the GA aims to minimize T; otherwise, it tries to minimize the number of blocked requests.

VII. Performance Evaluation of EON Provisioning With Dynamic Multicast Traffic

We evaluate the proposed multicast-capable RMSA with simulations using the 14-node NSFNET in Fig. 2 and the 28-node US Backbone in Fig. 4. Since the EON provisioning is a real-time service whose performance is sensitive to
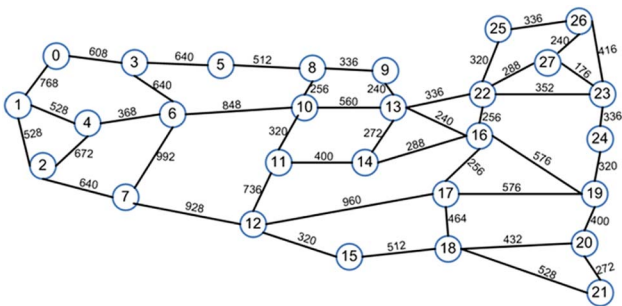

Fig. 4.   US Backbone topology with fiber lengths in kilometers marked on each link.

the computation time, we simulate only three heuristic algorithms, i.e., GA, MST, and SPT. We assume that the EON is deployed in the C band with an ~4.475 THz spectrum, and hence each fiber can accommodate $B = 358$ subcarrier slots. The multicast requests are generated according to a Poisson traffic model, with an average lifetime of each request of $1/\mu = 5$ time units. For the sizes of the multicast groups, we set the average $|D_i|$ of all requests as 3, 4, or 6. The other simulation parameters are the same as those in Table I.

Figure 5 shows the multicast request blocking probability results from simulations using the NSFNET topology. The results indicate that the GA approach offers the lowest request blocking probabilities for all simulation scenarios. This is because the GA can optimize the RMSA solutions of the requests with the objective defined in Eq. (31), while the MST and SPT algorithms can only optimize the routing paths but cannot optimize the RMSA jointly. A similar trend can be observed in Fig. 6 for the simulations with the US Backbone topology. In Figs. 5 and 6, we also observe that when we increase the average size of the multicast groups (i.e., $|D_i|$), the blocking probability reductions that the GA achieves over MST and SPT become smaller for high traffic loads (≥ 300 or 450 erlangs in NSFNET or US Backbone, respectively). This is because, when we increase
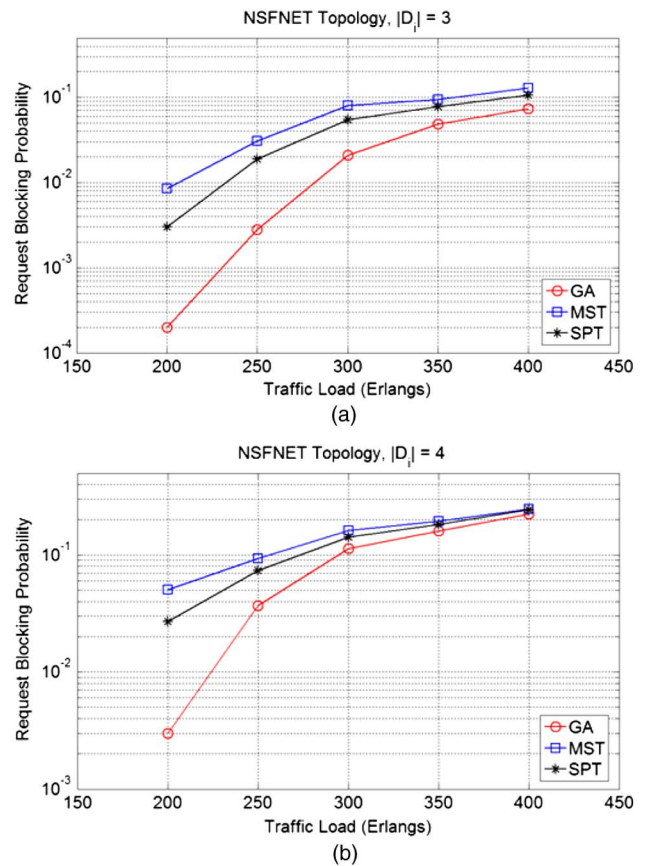

Fig. 5.   Multicast request blocking probability results from EON provisioning simulations using the NSFNET topology with (a) $|D_i| = 3$ and (b) $|D_i| = 4$.
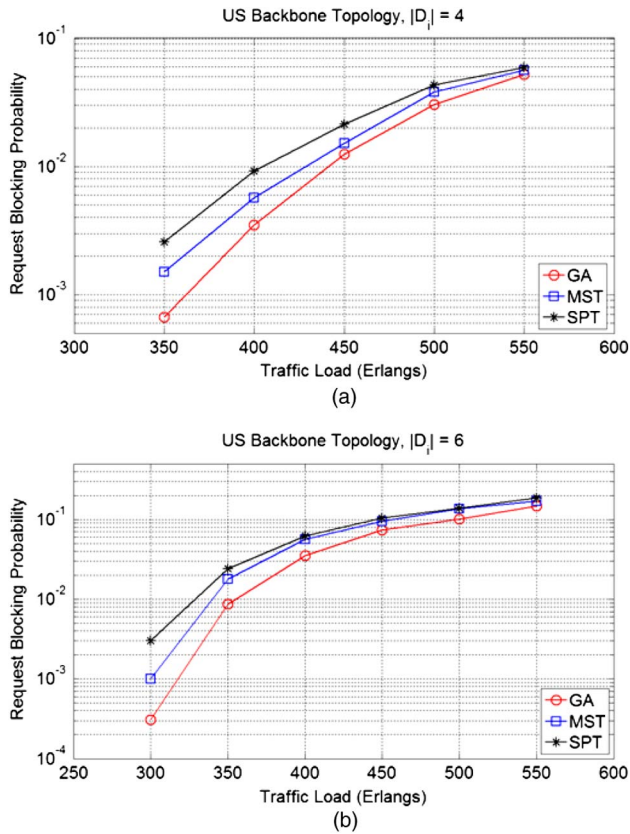
Fig. 6. Multicast request blocking probability results from EON provisioning simulations using the US Backbone topology with (a) $|D_i| = 4$ and (b) $|D_i| = 6$.

$|D_i|$, the network becomes more crowded and the GA has a smaller margin to perform the optimization.

It is interesting to observe that the blocking performance of SPT is better than that of MST with NSFNET in Fig. 5, while the relation is the opposite in Fig. 6 with US Backbone. We believe that this can be explained as follows. The light tree constructed by SPT has advantages in modulation-level assignments, as SPT makes sure that the longest path in it is the shortest, while the light tree from MST has a smaller number of links. The average length per link in NSFNET is 968.18 km, which is much longer than that in US Backbone (i.e., 466.49 km). This fact makes SPT's advantages in modulation-level assignments more significant.

VIII. DISCUSSION

In this work, we study all-optical multicasting over EONs that consist of multicast-capable nodes for optical splitting. The motivation of this work is that since O-OFDM achieves more flexible bandwidth management in the optical layer compared to the fixed-grid WDM, we expect future EONs to provide more efficient support to all-optical multicasting scenarios, especially for those induced by the emerging applications (e.g., e-Science [14]) whose traffic demands are usually huge and can have relatively large variations. As EONs allocate bandwidth with a finer granularity, the optical spectrum can be utilized

more wisely, and we can take one step forward toward seamless integration of the upper-layer applications and the optical-layer transmissions.

However, besides these advantages, we also want to point out that the enabling technologies for all-optical multicasting over EONs are still immature and not ready for practical deployment at this moment. For instance, the architecture of the multicast-capable EON nodes needs to be further investigated to make sure that the flexible-grid optical splitting can be achieved cost effectively. Considering that the multicast-capable EON node can be prohibitively expensive, our future work may need to study how to support multicast in EONs whose nodes are not all multicast capable. On the other hand, in order to simplify the problem, we assume that the majority of the impairments are from the long distance transmission between the nodes. Nevertheless, this assumption can limit our approaches' effectiveness. In our future work, we will implement a more sophisticated performance model, possibly based on the one that considers the physical layer impairments comprehensively [27].

IX. CONCLUSION

In this paper, we investigated the planning and provisioning of EONs with multicast traffic. For the static EON planning, we formulated two ILP models, the joint ILP and the separate ILP. The joint ILP optimized all multicast requests together, while the separate ILP optimized one request each time in a sequential way. To reduce the computational complexity of EON planning, we also proposed a highly efficient heuristic that was based on an adaptive GA with minimum solution revisits. The simulation results indicated that the ILPs and the GA provided more efficient EON planning than the existing multicast-capable RMSA algorithms that used the SPT and the MST. The results also showed that the GA obtained more efficient EON planning results than the separate ILP with much less running time, because it could optimize all multicast requests together in a highly efficient manner. The dynamic EON provisioning was then studied, and we demonstrated that the GA achieved lower request blocking probabilities than the benchmark algorithms using SPT and MST.

REFERENCES

[1] W. Shieh, X. Yi, and Y. Tang, "Transmission experiment of multi-gigabit coherent optical OFDM systems over 1000 km SSMF fiber," *Electron. Lett.*, vol. 43, pp. 183–185, Feb. 2007.

[2] J. Armstrong, "OFDM for optical communications," *J. Lightwave Technol.*, vol. 27, pp. 189–204, Feb. 2009.

[3] H. Takara, T. Goh, K. Shibahara, K. Yonenaga, S. Kawai, and M. Jinno, "Experimental demonstration of 400 Gb/s multi-flow,

multi-rate, multi-reach optical transmitter for efficient elastic spectral routing," in *37th European Conf. and Expo. on Optical Communications*, 2011, paper Tu.5.A.4.

[4] M. Jinno, B. Kozicki, H. Takara, A. Watanabe, Y. Sone, T. Tanaka, and A. Hirano, "Distance-adaptive spectrum resource allocation in spectrum-sliced elastic optical path network," *IEEE Commun. Mag.*, vol. 48, no. 8, pp. 138–145, Aug. 2010.

[5] A. Bocoi, M. Schuster, F. Rambach, M. Kiese, C. Bunge, and B. Spinnler, "Reach-dependent capacity in optical networks enabled by OFDM," in *Optical Fiber Communication Conf. and the Nat. Fiber Optic Engineers Conf.*, 2009, paper OMQ4.

[6] B. Kozicki, H. Takara, Y. Sone, A. Watanabe, and M. Jinno, "Distance-adaptive spectrum allocation in elastic optical path network (SLICE) with bit per symbol adjustment," in *Optical Fiber Communication Conf.*, 2010, paper OMU3.

[7] K. Christodoulopoulos, I. Tomkos, and E. Varvarigos, "Elastic bandwidth allocation in flexible OFDM-based optical networks," *J. Lightwave Technol.*, vol. 29, pp. 1354–1366, May 2011.

[8] Y. Wang, X. Cao, and Y. Pan, "A study of the routing and spectrum allocation in spectrum-sliced elastic optical path networks," in *Proc. IEEE INFOCOM*, Shanghai, Apr. 2011, pp. 1503–1511.

[9] L. Gong, X. Zhou, W. Lu, and Z. Zhu, "A two-population based evolutionary approach for optimizing routing, modulation and spectrum assignments (RMSA) in O-OFDM networks," *IEEE Commun. Lett.*, vol. 16, pp. 1520–1523, Sept. 2012.

[10] W. Lu, X. Zhou, L. Gong, and Z. Zhu, "Scalable network planning for elastic optical orthogonal frequency division multiplexing (OFDM) networks," in *8th Int. Symp. on Communication Systems, Networks & Digital Signal Processing (CSNDSP)*, Poznan, July 2012, pp. 1–4.

[11] Y. Sone, A. Hirano, A. Kadohata, M. Jinno, and O. Ishida, "Routing and spectrum assignment algorithm maximizes spectrum utilization in optical networks," in *37th European Conf. and Expo. on Optical Communications*, 2011, paper Mo.1.K.3.

[12] N. Sambo, F. Cugini, G. Bottari, P. Iovanna, and P. Castoldi, "Distributed setup in optical networks with flexible grid," in *37th European Conference and Exposition on Optical Communications*, OSA Technical Digest (CD). Washington, D.C.: Optical Society of America, 2011, paper We.10.P1.100.

[13] X. Wan, N. Hua, and X. Zheng, "Dynamic routing and spectrum assignment in spectrum-flexible transparent optical networks," *J. Opt. Commun. Netw.*, vol. 4, pp. 603–613, Aug. 2012.

[14] W. E. Johnston, "ESnet4: Networking for the future of DOE science," May 2008 [Online]. Available: https://es. net/assets/Uploads/ESnet4-Networking-for-the-Future-of-Science- 2008-05-05.NP.v1.pdf.

[15] L. Sahasrabuddhe and B. Mukherjee, "Light trees: Optical multicasting for improved performance in wavelength routed networks," *IEEE Commun. Mag.*, vol. 37, pp. 67–73, Feb. 1999.

[16] G. Rouskas, "Optical layer multicast: Rationale, building blocks, and challenges," *IEEE Network*, vol. 17, pp. 60–65, Feb. 2003.

[17] Z. Pan, H. Yang, J. Yang, J. Hu, Z. Zhu, J. Cao, K. Okamoto, S. Yamano, V. Akella, and B. Yoo, "Advanced optical-label routing system supporting multicast, optical TTL, and multimedia applications," *J. Lightwave Technol.*, vol. 23, pp. 3270–3281, Oct. 2005.

[18] R. Libeskind-Hadas and R. Melhem, "Multicast routing and wavelength assignment in multihop optical networks," *IEEE/ACM Trans. Netw.*, vol. 10, pp. 621–629, Oct. 2002.

[19] B. Chen and J. Wang, "Efficient routing and wavelength assignment for multicast in WDM networks," *IEEE J. Sel. Areas Commun.*, vol. 20, pp. 97–109, Jan. 2002.

[20] W. Hu and Q. Zeng, "Multicasting optical cross connects employing splitter-and-delivery switch," *IEEE Photon. Technol. Lett.*, vol. 10, pp. 970–972, July 1998.

[21] C. Lai and K. Bergman, "Broadband multicasting for wavelength-striped optical packets," *J. Lightwave Technol.*, vol. 30, pp. 1706–1718, June 2012.

[22] A. Gadkar, J. Plante, and V. Vokkarane, "Multicast overlay for high-bandwidth applications over WDM networks," *J. Opt. Commun. Netw.*, vol. 4, pp. 571–585, Aug. 2012.

[23] Q. Wang and L. Chen, "Performance analysis of multicast traffic over spectrum elastic optical networks," in *Optical Fiber Communication Conf.*, 2012, paper OTh3B.7.

[24] A. Ding and G. Poo, "A survey of optical multicast over WDM networks," *Comput. Commun.*, vol. 26, pp. 193–200, Feb. 2003.

[25] L. Kou, G. Markowsky, and L. Berman, "A fast algorithm for Steiner trees," *Acta Inf.*, vol. 15, pp. 141–145, 1981.

[26] Z. Yu, Y. Zhao, J. Zhang, X. Yu, B. Chen, and X. Lin, "Multicast routing and spectrum assignment in elastic optical networks," in *Asia Communications and Photonics Conf.*, 2012, paper AF3E.3.

[27] K. Christodoulopoulos, P. Soumplis, and E. Varvarigos, "Trading off transponders for spectrum in flexgrid networks," in *Optical Fiber Communication Conf. and the Nat. Fiber Optic Engineers Conf.*, 2013, paper OTu2A.3.

[28] A. Eira, J. Pedro, and J. Pires, "On the impact of optimized guard band assignment for superchannels in flexible grid optical networks," in *Optical Fiber Communication Conf. and the Nat. Fiber Optic Engineers Conf.*, 2013, paper OTu2A.5.

[29] X. Zhou, W. Lu, L. Gong, and Z. Zhu, "Dynamic RMSA in elastic optical networks with an adaptive genetic algorithm," in *Proc. GLOBECOM*, Anaheim, CA, Dec. 2012, pp. 1–6.

[30] J. Koza, *Genetic Programming: On the Programming of Computers by Means of Natural Selection*. Cambridge, Mass.: MIT, 1992.

[31] B. Miller, "Genetic algorithms, tournament selection, and effects of noise," *Complex Syst.*, vol. 9, pp. 193–212, July 1959.

[32] M. Srinivas and L. Patnaik, "Adaptive probabilities of crossover and mutation in genetic algorithms," *IEEE Trans. Syst. Man Cybern.*, vol. 24, pp. 656–667, Apr. 1994.

[33] "GLPK (GNU Linear Programming Kit)" [Online]. Available: http://www.gnu.org/software/glpk/.

[34] B. Mukherjee, *Optical WDM Networks*. New York: Springer, 2006.

[35] S. Aidarous, D. Proudfoot, and X. Dam, "Service management in intelligent networks," *IEEE Network*, vol. 4, pp. 18–24, Jan. 1990.

Long Gong received the B.S. degree from the Department of Electrical Engineering and Information Science, University of Science and Technology of China, Hefei, China, in 2012. He is working toward his M.S. degree in the same department. His research interest is elastic optical networks.

Xiang Zhou received the B.S. degree from the Department of Electrical Engineering, Hefei University of Technology, Hefei, China, in 2011. He is working toward his M.S. degree at the School of Information Science and Technology, University of Science and

Technology of China, Hefei, China. His research interest is elastic optical networks.

Xiahe Liu is an undergraduate student at the School of Information Science and Technology, University of Science and Technology of China, Hefei, China. She is expected to graduate in July 2013 and will pursue her M.S. degree in the same school beginning Sept. 2013. Her research interest is elastic optical networks.

Wenwen Zhao is an undergraduate student at the School of Information Science and Technology, University of Science and Technology of China, Hefei, China. She is expected to graduate in July 2013. Her research interest is elastic optical networks.

Wei Lu received the B.S. degree from the Department of Electrical Engineering, Zhejiang Normal University, Jinhua, China, in 2011. She is working toward her Ph.D. degree at the School of Information Science and Technology, University of Science and Technology of China, Hefei, China. Her research interest is elastic optical networks.

Zuqing Zhu (M'07-SM'12) received the Ph.D. degree from the Department of Electrical and Computer Engineering, University of California, Davis, in 2007. From July 2007 to January 2011, he worked in the Service Provider Technology Group of Cisco Systems, San Jose, as a senior R&D engineer. In January 2011, he joined the University of Science and Technology of China (USTC), where he currently is an Associate Professor. His research interests are elastic optical networks and energy-efficient optical networks. He has published more than 80 papers in peer-reviewed journals and conferences of IEEE, IEE, and OSA. He has been in the technical program committees (TPCs) of INFOCOM, ICC, GLOBECOM, ICCCN, etc. He was a guest editor of the IEEE Network special issue on "Optical Networks in Cloud Computing." He is also an editorial board member of the Elsevier *Journal of Optical Switching and Networking* (OSN), Springer *Telecommunication Systems* journal (TSMJ), Wiley *European Transactions on Emerging Telecommunications Technologies* (ETT), etc. He is a Senior Member of IEEE and a Member of OSA.